Magnetic properties of a loop containing N weak links

1992 J. Phys.: Condens. Matter 4 2253

(http://iopscience.iop.org/0953-8984/4/9/019)

J. Phys.: Condens. Matter 4 (1992) 2253–2262. Printed in the UK

Magnetic properties of a loop containing N weak links

Daniel Spišák and Peter Kopčanský
Institute of Experimental Physics, Slovak Academy of Sciences, Solovjevova 47, 043 53 Košice, Czechoslovakia

Received 9 April 1991, in final form 5 September 1991

Abstract. The ring with N weak links in the magnetic field is examined. The exact form of the partition function of the model was obtained, what permits one to evaluate all the thermodynamic characteristics of the model. We concentrated on the heat capacity and particularly on the susceptibility, which exhibits quite remarkable features in the finite-size limit. In addition, the influence of the weak-link strength distribution is explored.

1. Introduction

The aim of this paper is to investigate the magnetic properties of the superconducting circuit with N Josephson junctions. Arrangements such as these have been studied intensively ever since Jaklevic *et al* [1] have developed a DC superconducting quantum interference device (SQUID) consisting of two parallel Josephson junctions in circuit. Similarly, devices made from a symmetric circuit with four Josephson junctions have been pursued [2, 3]. The flux dynamics of ring containing five weak links were numerically studied in [4].

Our approach starts from the studies investigating layers of weak bound granular superconductors in the magnetic field. These systems can be well described by the frustrated XY model (see, e.g., [5]), in which the frustration is induced by the magnetic field. Moreover, in recent years, two-dimensional arrays of superconducting grains joined through weak links have been prepared [6–9] by the modern photomicrolithographic techniques. Likewise, spherical superconductive grains of the size about 1 μm dispersed in a polymerized ferrofluid composite exposed to a magnetic field form a ring-shaped circuit [10] and weak links between grains might arise.

The remainder of the paper is organized as follows. The description of the model and the main results are presented in section 2, and section 3 deals with some comments on the validity of our approach.

2. The model

Consider an isolated closed loop created by the superconductive grains connected through Josephson junctions. These grains are assumed to be small owing to the coherent length of a bulk superconductor; thus each grain can be controlled by one dynamic

0953-8984/92/092253 + 10 $04.50

variable φ_i. The high-capacitance approximation, in the framework of which the fluctuation effects may be neglected, allows one to describe the system by the above-mentioned frustrated XY model (sometimes called the plane rotator model) with the Hamiltonian

$$H = -\sum_{j=1}^{N} J_j \cos(\varphi_j - \varphi_{j+1} - A_j) \qquad \varphi_{N+1} = \varphi_1 \tag{2.1}$$

where J is coupling energy for the tunnelling junction between the jth and the $(j+1)$th grain depending on a medium via which the weak connection is induced; the phase angle

$$A_j = \frac{2\pi}{\phi_0} \int_j^{j+1} \boldsymbol{A} \cdot \mathrm{d}\boldsymbol{l} \tag{2.2}$$

ensuring the gauge invariance, $\boldsymbol{A}$ is the vector potential, $\phi_0 = h/2e$ is the magnetic flux quantum and the integral is taken along a line joining the centres of jth and $(j+1)$th grains. In the case of a closed circuit, one gets

$$\sum_{j=1}^{N} A_j = \frac{2\pi}{\phi_0} \oint \boldsymbol{A} \cdot \mathrm{d}\boldsymbol{l} = 2\pi f \tag{2.3}$$

regardless of the arrangement of grains along the loop, where the frustration $f = \phi/\phi_0$ as a number of magnetic flux quantum through the area of circuit was introduced. Non-integer values of f mean that there is no frustration in the system or, in other words, it is not possible for the system to attain a state which minimalizes all the bondings at the same time. From equations (2.1) and (2.3) it is clear that it suffices to restrict our considerations to $-0.5 \leqslant f < 0.5$ and, as the exchange $f \to -f$ amounts to a change in the direction of the external magnetic field, only the interval $0 \leqslant f \leqslant 0.5$ is examined below. This means, presumably, that the model manifests an oscillatory behaviour in the magnetic field because of quantification of the magnetic flux through the loop area.

The thermodynamic properties of the system are determined by the classical partition function (with $\beta = 1/k_B T$)

$$Z = \int_0^{2\pi} \int_0^{2\pi} \ldots \int_0^{2\pi} \exp(-\beta H) \prod_{j=1}^{N} \frac{\mathrm{d}\varphi_j}{2\pi} \tag{2.4}$$

which provides the free energy

$$F = -(1/\beta) \ln Z. \tag{2.5}$$

In terms of F the isothermal differential susceptibility reads

$$\chi = -(1/\mu_0)(\partial^2 F/\partial H^2)_T \tag{2.6}$$

and the specific heat capacity is given by

$$C_v = -T(\partial^2 F/\partial T^2)_v. \tag{2.7}$$

Substituting equation (2.1) into equation (2.4) and utilizing the mathematical identity known as the Jacobi–Anger expansion

$$\exp(J \cos x) = \sum_{n=-\infty}^{\infty} I_n(J) \exp(\mathrm{i}nx) \tag{2.8}$$

where I_n is the modified nth-order Bessel function, after some algebra one gets the statistical partition sum of N Josephson junctions:

$$Z_N = \sum_{n=-\infty}^{\infty} \prod_{j=1}^{N} I_n(\beta J_j) \exp(\mathrm{i}2\pi f n). \tag{2.9}$$

This result holds for a closed circuit of arbitrary shape. In what follows, a circular

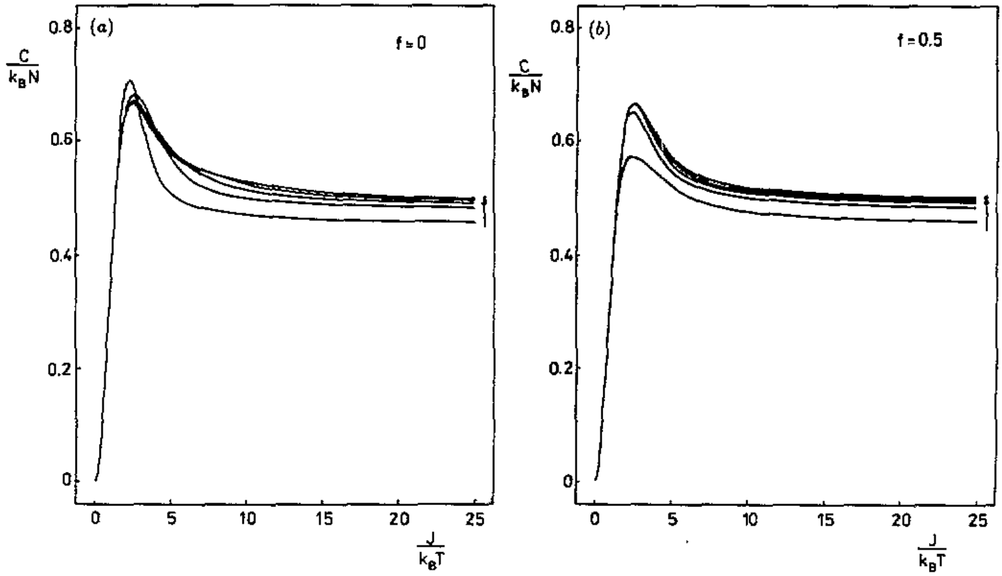

Figure 1. The plot of the specific heat capacity versus the inverse temperature for frustration (*a*) $f = 0$ and (*b*) $f = 0.5$. The arrow indicates the increasing number N of the weak links in the circuit from 10 to 50.

loop will be assumed for concreteness, and the typical linear size of each grain is set equal to $2a$. Then the area of loop for a large number N of grains is

$$S(N) = (Na)^2/\pi. \tag{2.10}$$

Of course, if one takes an interest in the behaviour of low-body systems, then equation (2.10) can be re-expressed depending on the shape of the grains. For example, if a circular loop containing not too many spherical grains is considered, then the area limited by the interior contour of the circuit (here it is supposed that the penetration depth of a grain is much less than a) is

$$S(N) = [N/\tan(\pi/N) - \pi(N-2)/2]a^2$$

which gives equation (2.10) for large N.

Before exploring the thermodynamic characteristics of the model due to equation (2.9), we look for a moment at the special case $T = 0$. Now the current conservation requires that all the phase differences are identical [11]:

$$\varphi_j - \varphi_{j+1} = 2\pi m/N \qquad m = 0, \pm 1, \pm 2, \ldots$$

for regularly distributed grains. This straight away yields for the free energy

$$F = -\sum_{j=1}^{N} J_j \cos\left(\frac{2\pi}{N}(m - f)\right). \tag{2.11}$$

From here according to equation (2.6) we have the susceptibility

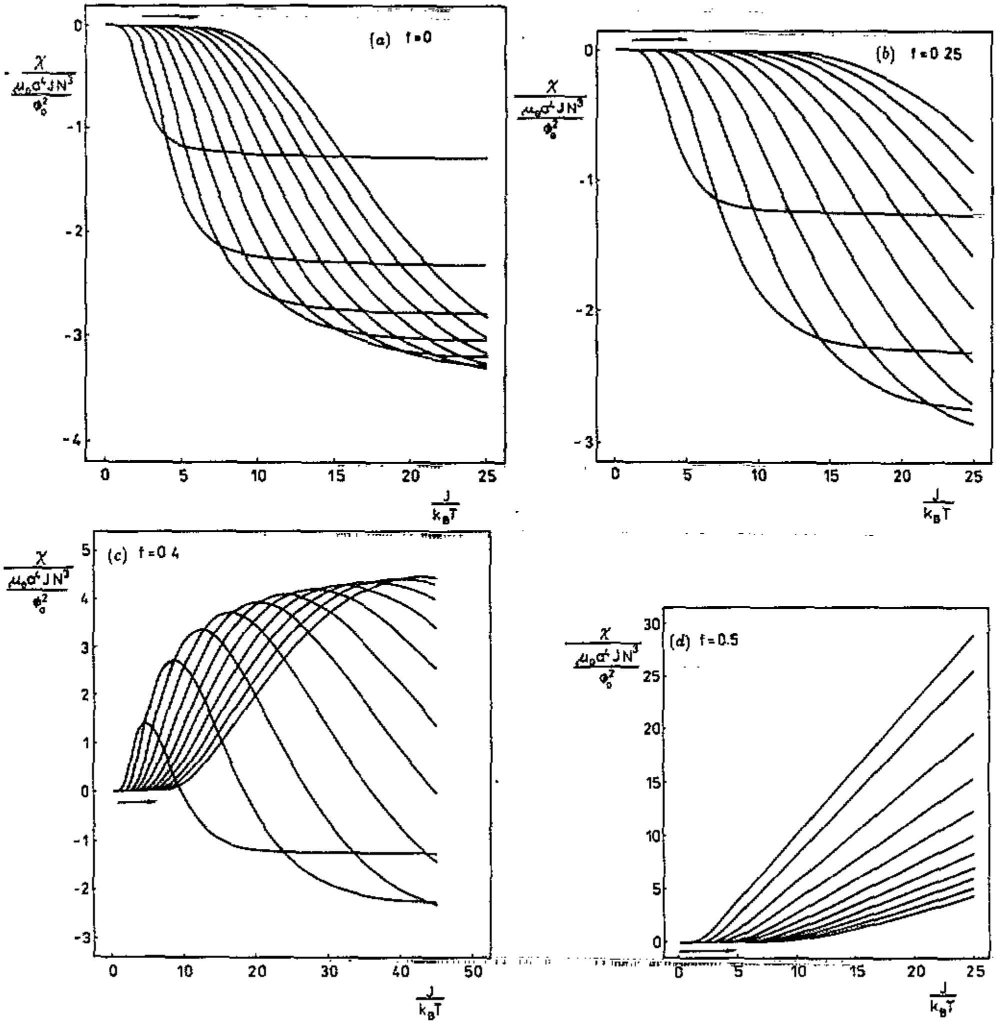

Figure 2. The reduced differential susceptibility of the circuit with 10 up to 110 grains versus the inverse temperature for frustration (*a*) $f = 0$, (*b*) $f = 0.25$, (*c*) $f = 0.4$ and (*d*) $f = 0.5$. The arrow indicates the increase in number of grains.

$$\chi = \left(-\mu_0[2\pi S(N)]^2 \sum_{j=1}^{N} J_j \Big/ \phi_0^2 N^2\right) \cos\left(\frac{2\pi}{N}(m-f)\right). \tag{2.12}$$

The asymptotic behaviour $\chi \sim N^3$ is a typical feature for such systems [12]. Further, for large N the differential susceptibility does not depend on the magnetic field whether frustration occurs or not.

Now let us proceed to the study of the finite temperature properties of the model.

2.1. *The ideal arranged circuit*

First we turn to an idealized situation of the perfectly homogeneous system with all the coupling energies J_j the same and denoted as J. The partition sum can be recast:

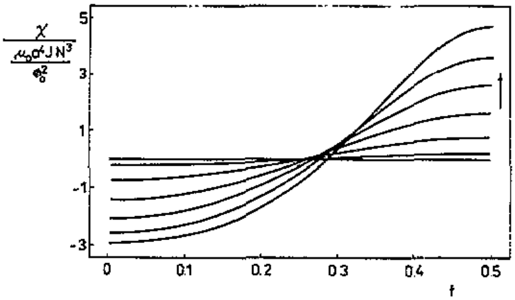

Figure 3. The plot of the reduced differential susceptibility of the 100 weak links in the loop versus frustration for various temperatures $J/k_BT = 3, 6, 9, \ldots, 24$ in the arrow direction.

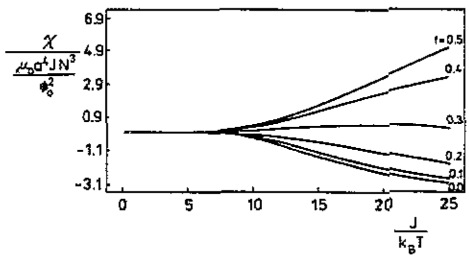

Figure 4. The temperature dependence of the 100-grain loop susceptibility for various values of frustration.

$$Z_N = \sum_{n=-\infty}^{\infty} I_n^N(\beta J)\exp(\mathrm{i}2\pi f n). \tag{2.13}$$

Although we focus our attention primarily on the magnetic properties, we shall also mention the heat capacity. The heat capacity dependence on the temperature and number N of grains for two frustrations $f = 0$ and $f = 0.5$ is depicted in figure 1(a) and 1(b), respectively. The heat capacity of the closed loop reaches that of a linear chain of grains as N increases. The partition function of the linear chain may be obtained by integrating equation (2.4) successively over φ_1 to φ_N without the constraint $\varphi_1 = \varphi_N$, which yields

$$Z_N = I_0^{N-1}(\beta J) \tag{2.14}$$

and the heat capacity of the chain per particle can be inferred [13]:

$$C_N/k_BN = [(N-1)/N](J\beta)^2\{1 - I_1(\beta J)/J\beta I_0(\beta J) - [I_1(\beta J)/I_0(\beta J)]^2\}. \tag{2.15}$$

That is to say, the heat capacity of a closed circuit formed by Josephson junctions does not depend on the magnetic field in the thermodynamic limit; nonetheless for not too many grains (roughly up to 50) an effect of the magnetic field is observable.

On the other hand, the behaviour of the susceptibility of this simple model might seem to be fairly surprising. In regular two-dimensional arrays, where a discontinuous variation in the nature of transition and formation of superlattices as the frustration is varied is expected [5], the properties of system have to be examined for any frustration of its own. Now the frustration plays the role of a continuous parameter. The susceptibility versus temperature for $f = 0$, 0.25, 0.4 and 0.5 is shown in figures 2(a), 2(b), 2(c) and 2(d), respectively. A more detailed analysis revealed that three regions in the temperature dependence of the susceptibility can be established.

In region I, for $0 \leqslant f \leqslant 0.25$ the model exhibits a pure diamagnetic behaviour at any temperature.

In region II, for $0.25 < f < 0.5$ a temperature exists, depending on the size of system, at which the low-temperature diamagnetic susceptibility changes into the high-temperature paramagnetic susceptibility (this is also evident from figures 3 and 4).

In region III, in the fully frustrated system $f = 0.5$, when the condition of 2π periodicity is violated mainly because $\Sigma_{j=1}^N A_j = \pi$, the susceptibility is paramagnetic in the

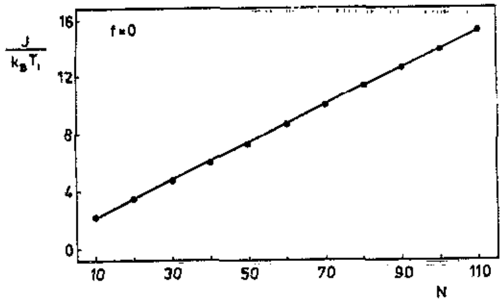

Figure 5. The plot of the susceptibility inflection point temperature T_i obtained from figure 2(a) versus the number of weak links for $f = 0$.

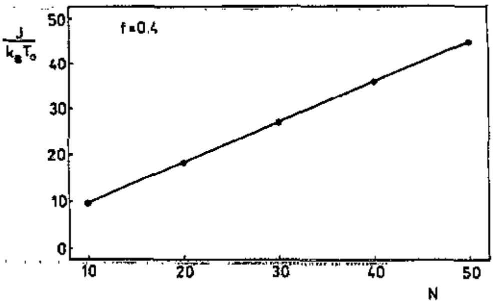

Figure 6. The plot of the zero susceptibility temperature T_0 obtained from figure 2(c) versus the number of weak links for $f = 0.4$.

whole temperature range. As is visible in figure 2(d) the susceptibility diverges for $T \rightarrow 0$ despite the finiteness of the system in this case and, on the contrary, for an infinite system the divergent behaviour ceases (see appendix).

Of course, finite-size effects need not be neglected. In the first frustration region a temperature T_i, the temperature of the locus of the susceptibility inflection point, is introduced and, in figure 5, T_i for 10–110 weak links N is presented for the case $f = 0$. The inverse proportion observed in figure 5 was obtained also for other values of frustration from this interval, which testifies to the loss of the diamagnetic behaviour of the circuit in the thermodynamic limit.

Similarly, for f between 0.25 and 0.5 the temperature T_0 can be assigned to the zero-susceptibility value as a characteristic of the circuit. A typical dependence T_0 on number of grains for $f = 0.4$ is shown in figure 6. As is seen, $T_0 \sim 1/N$ again, according to the preceding conclusion that there is no diamagnetic range for susceptibility for large N.

In the thermodynamic limit, when the concrete shape of the circuit is irrelevant, it will suffice to calculate the initial susceptibility of the infinite linear chain of Josephson junctions. To do this in the easiest way the fluctuation–dissipation theorem for the susceptibility can be utilized:

$$\chi = \beta \sum_{r=0}^{\infty} \langle \cos(\varphi_0 - \varphi_r) \rangle \tag{2.16}$$

where the correlation function $\langle \cos(\varphi_0 - \varphi_r) \rangle$ between the two phases at a distance r can be calculated in the same manner as the statistical function (2.9). This results in

$$\langle \cos(\varphi_0 - \varphi_r) \rangle = \sum_{n=-\infty}^{\infty} I_n^{N-r}(\beta J) I_{n+1}^{r}(\beta J) \Big/ \sum_{n=-\infty}^{\infty} I_n^N(\beta J). \tag{2.17}$$

Equations (2.16) and (2.17) yield in the thermodynamic limit the divergence just for $T = 0$ as is expected for a 1D system.

2.2. *The disorder circuit*

Real structures despite the afore-mentioned discussion are not characterized by identical Josephson junctions; in other words, a certain distribution of the coupling energies $\{J_i\}$

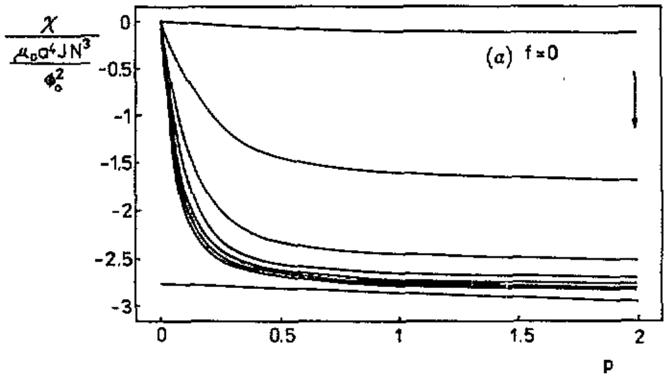

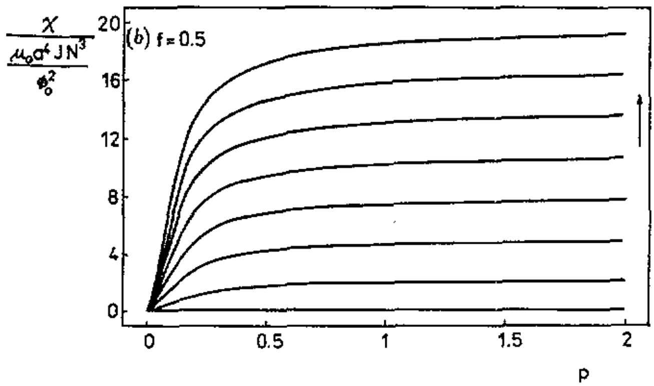

Figure 7. The reduced differential susceptibility of 30 weak links as a function of parameter p (see equation (2.18)) for (*a*) $f = 0$ and (*b*) $f = 0.5$. The arrow indicates the increase of $J/k_BT = 3, 6, 9, \ldots, 24$. The straight line in (*a*) corresponds to the zero-temperature limit.

is always present because of, for example, the various size of grains between which the weak link is realized. Therefore it is of importance to explore how the disorder of the system modifies the above results.

First the simplest case with only one weak link which varies its coupling energy is considered:

$$\begin{aligned} J_j &= J \\ J_k &= pJ \end{aligned} \qquad j = 1, 2, \ldots, k-1, k+1, \ldots N. \tag{2.18}$$

This approximation corresponds to the gradual disconnection of the loop as p tends to zero. Using equations (2.9) and (2.6) and taking equation (2.18) into account, figures 7(*a*) and 7(*b*) were obtained, where the susceptibilities for $f = 0$ and 0.5, respectively, are depicted versus the parameter p. The line in figure 7(*a*) pertains to the zero temperature and comes from equations (2.11) and (2.6). Under any circumstances the susceptibility increases proportionately to p for small p and rapidly saturates for $p > 1$.

Finally we examined the influence of the coupling constant distribution on the

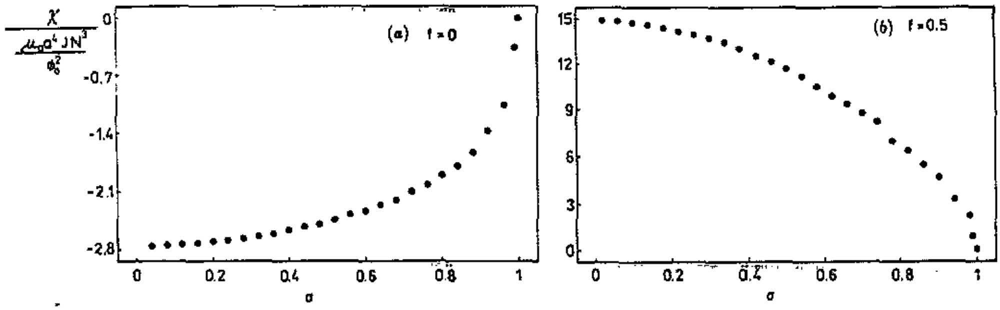

Figure 8. The reduced differential susceptibility of 30 weak links with $\{J_i\}$ distributed according to the box-shaped distribution as a function of the disorder parameter σ for $J/k_BT = 20$ and $(a)\, f = 0$ and $(b)\, f = 0.5$.

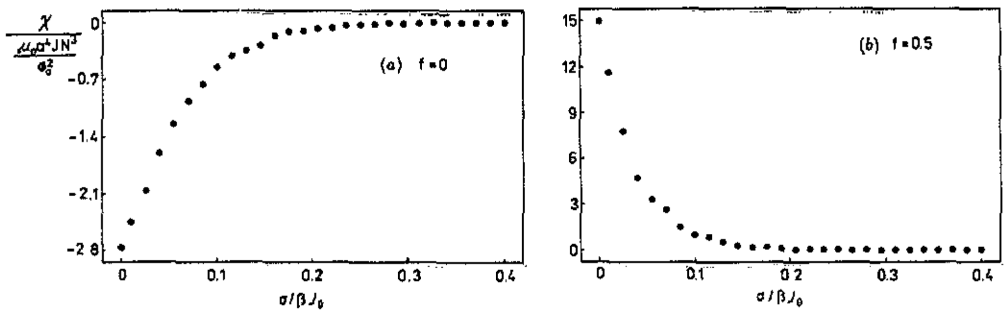

Figure 9. The same as in figure 8 but for the log–normal distribution.

magnetic properties of the model. We have chosen two suitable distribution functions:

(1) the box-shaped distribution

$$P(J) = \begin{cases} 1/2J_0\sigma & J_0(1-\sigma) < J < J_0(1+\sigma) \\ 0 & \text{otherwise} \end{cases} \tag{2.19}$$

(2) the log–normal distribution

$$P(J) = (1/\sqrt{2\pi\sigma}J) \exp[-\ln^2(J/J_0)/2\sigma] \tag{2.20}$$

where J_0 and σ denote the usual appropriate distribution parameters in both cases.

As the direct calculation of the configuration integrals cannot be executed explicitly we resorted to computer simulation. We carried out the susceptibility average through 200 realizations with given distributions for the circuit composed of 30 grains for $f = 0$ and 0.5 at the temperature $J\beta = 20$. The results for the box-shaped distribution of coupling energies are presented in figures 8(a) and 8(b) and for the log–normal distribution in figures 9(a) and 9(b). In both cases the susceptibility decreases considerably with growing disorder and vanishes when values J near zero are reached statistically, in agreement with preceding results.

3. Final remarks

In this paper the simplified model of a ring with N weak links has been studied in the high-capacitance limit. As to the discussion about the validity of the high-capacitance limit for a chain made up of photolithographic junctions the reader is referred to [14]. Of course, for too small grains this approximation no longer holds and including the capacitance term in the Hamiltonian becomes necessary. This leads to solving the quantum mechanics system.

The inductance effects, in turn, are not taken into account, which fails of course for large loops. The estimation of the upper number of weak links in the circuit follows from the relation $\frac{1}{2}LI_c^2 \simeq J$ and it yields $N_{max} \simeq 2\hbar/\mu_0 eaI_c$. Substituting a typical value for the critical current I_c through the Josephson junction of about 1 μA [7, 8] and a grain radius $a \simeq 1$ μm, one can estimate that $N_{max} \simeq 10^4$.

We believe that, it might be intriguing to undertake an experimental investigation of such a model to compare the results presented above with real results. The best observable phenomena are to be found for the strongly homogeneous sample for instance and other similar preliminary predictions may be made with respect to the conclusions of the article. The utilization of N weak-link elements for the measurement of weak magnetic fields and low temperatures is also conceivable.

Appendix

In this appendix we try to elucidate the divergence of the susceptibility for the fully frustrated model $f = 0.5$. The ratio of the sums in the susceptibility obtained from equations (2.5), (2.6) and (2.13) given by

$$\chi = -\frac{8\pi\mu_0 S^2}{\phi_0^2\beta} \sum_{k=1}^{\infty} (-1)^k k^2 I_k^N(\beta J) \Big/ \sum_{k=-\infty}^{\infty} (-1)^k I_k^N(\beta J) \tag{A1}$$

can be estimated in the limit of large N as follows:

$$\begin{aligned}\chi &\approx -(1/\beta)[-I_1^N(\beta J) + 4I_2^N(\beta J) - \ldots]/[I_0^N(\beta J) - 2I_1^N(\beta J) + \ldots] \\ &\approx 1/\beta\, [I_1(\beta J)/I_0(\beta J)]^N / \{1 - 2[I_1(\beta J)/I_0(\beta J)]^N\}\end{aligned} \tag{A2}$$

where only the leading terms of the sums were left. In the limit of low temperatures the Bessel function of imaginary argument reduces to

$$I_k(x) = \exp(-k^2/2x)/\sqrt{2\pi x} \qquad x \to \infty \tag{A3}$$

so that the susceptibility may be rewritten as

$$\chi = 1/\beta\; 1/[\exp(N/2\beta J) - 2] \qquad \beta \to \infty. \tag{A4}$$

Now, if the thermodynamic limit is taken, the susceptibility vanishes. Conversely, for finite N a critical temperature

$$T_c = (J \ln 4)/k_B N \tag{A5}$$

can be found when the susceptibility diverges in perfect consistency with figure 2(d), although the divergence region around T_c is not displayed as the precision of our computer calculations for large N and β is beyond the necessary accuracy. For $T < T_c$ we suppose an oscillatory character of susceptibility due to sign alternation in equation (A1).

References

[1] Jaklevic R C, Lambe L, Silver A H and Mercerau J E 1964 *Phys. Rev. Lett.* **12** 159
[2] Fink H J, Grünfeld S M and Roberts S M 1987 *Phys. Rev.* B **36** 74
[3] McDonald D G 1984 *Appl. Phys. Lett.* **45** 1243
[4] Blackburn J A 1984 *J. Appl. Phys.* **56** 1477
[5] Chung J S, Lee K H and Stroud D 1989 *Phys. Rev.* B **40** 6570
José J V, Kadanoff L P, Kirkpatrick S and Nelson D R 1977 *Phys. Rev.* B **16** 1217
Kosterlitz J M and Thouless D J 1973 *J. Phys. C: Solid State Phys.* **6** 1181
Choi M Y and Doniach S 1985 *Phys. Rev.* B **31** 4516
[6] Webb R A, Voss R F, Grinstein G and Horn P M 1983 *Phys. Rev. Lett.* **51** 690
[7] van Wess B J, van Zant H S J and Mooij J E 1987 *Phys. Rev.* B **35** 7291
[8] Carini J P 1988 *Phys. Rev.* B **38** 63
[9] Rzchowski M S, Benz S P, Tinkham M and Lobb C J 1983 *Phys. Rev.* B **42** 2041
[10] Kopčanský P, Černák J and Legéň G 1990 *CS Patent Specification* PV-3512/90
[11] Ebner C and Stroud D 1985 *Phys. Rev.* B **31** 165
[12] Rammal R, Lubensky T C and Tolouse G 1983 *Phys. Rev.* B **27** 2820
[13] Ami S and Kleinert H 1986 *Phys. Rev.* B **33** 4692
[14] Bradley R M and Doniach S 1984 *Phys. Rev.* B **30** 1138